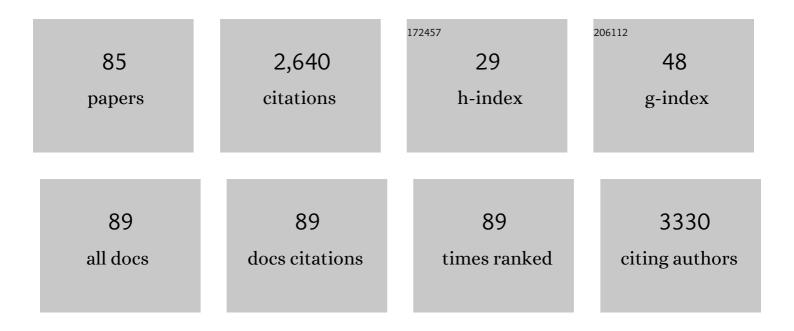
List of Publications by Year in descending order

Source: https://exaly.com/author-pdf/5856877/publications.pdf Version: 2024-02-01



OLE L MUNK

#	Article	IF	CITATIONS
1	Brain-first versus body-first Parkinson's disease: a multimodalÂimaging case-control study. Brain, 2020, 143, 3077-3088.	7.6	398
2	Imaging acetylcholinesterase density in peripheral organs in Parkinson's disease with 11C-donepezil PET. Brain, 2015, 138, 653-663.	7.6	135
3	Brain metabolism of13N-ammonia during acute hepatic encephalopathy in cirrhosis measured by positron emission tomography. Hepatology, 2006, 43, 42-50.	7.3	111
4	In Vivo Imaging of Human ¹¹ C-Metformin in Peripheral Organs: Dosimetry, Biodistribution, and Kinetic Analyses. Journal of Nuclear Medicine, 2016, 57, 1920-1926.	5.0	106
5	Subchronic Haloperidol Downregulates Dopamine Synthesis Capacity in the Brain of Schizophrenic Patients In Vivo. Neuropsychopharmacology, 2003, 28, 787-794.	5.4	105
6	Dynamic FDC-PET is useful for detection of cholangiocarcinoma in patients with PSC listed for liver transplantation. Hepatology, 2006, 44, 1572-1580.	7.3	87
7	The use of PET/CT scanning technique for 3D visualization and quantification of real-time soil/plant interactions. Plant and Soil, 2012, 352, 113-127.	3.7	83
8	Identifying hypoxia in human tumors: A correlation study between ¹⁸ F-FMISO PET and the Eppendorf oxygen-sensitive electrode. Acta Oncológica, 2010, 49, 934-940.	1.8	74
9	[11C]-Labeled Metformin Distribution in the Liver and Small Intestine Using Dynamic Positron Emission Tomography in Mice Demonstrates Tissue-Specific Transporter Dependency. Diabetes, 2016, 65, 1724-1730.	0.6	69
10	Hepatic encephalopathy is associated with decreased cerebral oxygen metabolism and blood flow, not increased ammonia uptake. Hepatology, 2013, 57, 258-265.	7.3	63
11	Effect of intratumoral heterogeneity in oxygenation status on FMISO PET, autoradiography, and electrode Po2 measurements in murine tumors. International Journal of Radiation Oncology Biology Physics, 2005, 62, 854-861.	0.8	56
12	Obeticholic acid improves hepatic bile acid excretion in patients with primary biliary cholangitis. Journal of Hepatology, 2021, 74, 58-65.	3.7	54
13	Effect of age on markers for monoaminergic neurons of normal and MPTP-lesioned rhesus monkeys: A multi-tracer PET study. NeuroImage, 2006, 30, 26-35.	4.2	50
14	Branched-chain amino acids increase arterial blood ammonia in spite of enhanced intrinsic muscle ammonia metabolism in patients with cirrhosis and healthy subjects. American Journal of Physiology - Renal Physiology, 2011, 301, G269-G277.	3.4	49
15	Kinetics of the metabolism of four PET radioligands in living minipigs. Nuclear Medicine and Biology, 2001, 28, 97-104.	0.6	43
16	Prognostic modeling for patients with colorectal liver metastases incorporating FDG PET radiomic features. European Journal of Radiology, 2019, 113, 101-109.	2.6	42
17	In Vivo Imaging of Human Acetylcholinesterase Density in Peripheral Organs Using ¹¹ C-Donepezil: Dosimetry, Biodistribution, and Kinetic Analyses. Journal of Nuclear Medicine, 2014, 55, 1818-1824.	5.0	40
18	Hepatobiliary transport kinetics of the conjugated bile acid tracer 11C-CSar quantified in healthy humans and patients by positron emission tomography. Journal of Hepatology, 2017, 67, 321-327.	3.7	40

#	Article	IF	CITATIONS
19	[<i>N</i> -Methyl- ¹¹ C]Cholylsarcosine, a Novel Bile Acid Tracer for PET/CT of Hepatic Excretory Function: Radiosynthesis and Proof-of-Concept Studies in Pigs. Journal of Nuclear Medicine, 2012, 53, 772-778.	5.0	38
20	MDMA-evoked changes in [11C]raclopride and [11C]NMSP binding in living pig brain. Synapse, 2004, 53, 222-233.	1.2	36
21	Glucose metabolism in small subcortical structures in Parkinson's disease. Acta Neurologica Scandinavica, 2012, 125, 303-310.	2.1	36
22	Assessing hypoxia in animal tumor models based on pharmocokinetic analysis of dynamic FAZA PET. Acta OncolA³gica, 2010, 49, 922-933.	1.8	35
23	11C-methionine PET, a novel method for measuring regional salivary gland function after radiotherapy of head and neck cancer. Radiotherapy and Oncology, 2004, 73, 289-296.	0.6	34
24	Mapping the amphetamine-evoked changes in [11C]raclopride binding in living rat using small animal PET: Modulation by MAO-inhibition. NeuroImage, 2007, 35, 38-46.	4.2	34
25	Clinical feasibility and impact of fully automated multiparametric PET imaging using direct Patlak reconstruction: evaluation of 103 dynamic whole-body 18F-FDG PET/CT scans. European Journal of Nuclear Medicine and Molecular Imaging, 2021, 48, 837-850.	6.4	34
26	Individual radiation response of parotid glands investigated by dynamic 11C-methionine PET. Radiotherapy and Oncology, 2006, 78, 262-269.	0.6	33
27	Hepatic uptake and metabolism of galactose can be quantified in vivo by 2-[¹⁸ F]fluoro-2-deoxygalactose positron emission tomography. American Journal of Physiology - Renal Physiology, 2008, 295, G27-G36.	3.4	33
28	Dynamic 2-[18 F]fluoro-2-deoxy- d -glucose positron emission tomography of liver tumours without blood sampling. European Journal of Nuclear Medicine and Molecular Imaging, 2000, 27, 407-412.	6.4	32
29	Peripheral benzodiazepine receptors in the brain of cirrhosis patients with manifest hepatic encephalopathy. European Journal of Nuclear Medicine and Molecular Imaging, 2006, 33, 810-816.	6.4	31
30	Mapping α ₂ Adrenoceptors of the Human Brain with ¹¹ C-Yohimbine. Journal of Nuclear Medicine, 2015, 56, 392-398.	5.0	31
31	A method to estimate dispersion in sampling catheters and to calculate dispersion-free blood time-activity curves. Medical Physics, 2008, 35, 3471-3481.	3.0	28
32	Human 13N-ammonia PET studies: the importance of measuring 13N-ammonia metabolites in blood. Metabolic Brain Disease, 2010, 25, 49-56.	2.9	27
33	Hepatobiliary Secretion Kinetics of Conjugated Bile Acids Measured in Pigs by ¹¹ C-Cholylsarcosine PET. Journal of Nuclear Medicine, 2016, 57, 961-966.	5.0	25
34	Impulse-response function of splanchnic circulation with model-independent constraints: theory and experimental validation. American Journal of Physiology - Renal Physiology, 2003, 285, G671-G680.	3.4	24
35	Whole-Body Biodistribution, Dosimetry, and Metabolite Correction of [¹¹ C]Palmitate: A PET Tracer for Imaging of Fatty Acid Metabolism. Molecular Imaging, 2017, 16, 153601211773448.	1.4	23
36	Loss of metabolites from monkey striatum during PET with FDOPA. Synapse, 2001, 41, 212-218.	1.2	22

#	Article	IF	CITATIONS
37	Inhibition of [11C]mirtazapine binding by α2-adrenoceptor antagonists studied by positron emission tomography in living porcine brain. Synapse, 2006, 59, 463-471.	1.2	21
38	Backflux of ammonia from brain to blood in human subjects with and without hepatic encephalopathy. Metabolic Brain Disease, 2009, 24, 237-242.	2.9	21
39	Tracer input for kinetic modelling of liver physiology determined without sampling portal venous blood in pigs. European Journal of Nuclear Medicine and Molecular Imaging, 2011, 38, 263-270.	6.4	21
40	Intravenous and oral copper kinetics, biodistribution and dosimetry in healthy humans studied by [64Cu]copper PET/CT. EJNMMI Radiopharmacy and Chemistry, 2020, 5, 15.	3.9	21
41	A PET Tracer for Renal Organic Cation Transporters, ¹¹ C-Metformin: Radiosynthesis and Preclinical Proof-of-Concept Studies. Journal of Nuclear Medicine, 2016, 57, 615-621.	5.0	20
42	Hepatic exposure of metformin in patients with nonâ€alcoholic fatty liver disease. British Journal of Clinical Pharmacology, 2019, 85, 1761-1770.	2.4	19
43	Distribution of PK11195 binding sites in porcine brain studied by autoradiography in vitro and by positron emission tomography. Synapse, 2006, 59, 418-426.	1.2	18
44	Radiosynthesis of <i>N</i> - ¹¹ C-Methyl-Taurine–Conjugated Bile Acids and Biodistribution Studies in Pigs by PET/CT. Journal of Nuclear Medicine, 2016, 57, 628-633.	5.0	18
45	Metformin does not affect postabsorptive hepatic free fatty acid uptake, oxidation or resecretion in humans: A 3â€month placeboâ€controlled clinical trial in patients with type 2 diabetes and healthy controls. Diabetes, Obesity and Metabolism, 2018, 20, 1435-1444.	4.4	18
46	Capillaries within compartments: microvascular interpretation of dynamic positron emission tomography data. Journal of Theoretical Biology, 2003, 225, 127-141.	1.7	17
47	Hepatic Blood Perfusion Measured by 3-Minute Dynamic ¹⁸ F-FDG PET in Pigs. Journal of Nuclear Medicine, 2011, 52, 1119-1124.	5.0	17
48	Determination of regional flow by use of intravascular PET tracers: microvascular theory and experimental validation for pig livers. Journal of Nuclear Medicine, 2003, 44, 1862-70.	5.0	17
49	Normal values for 18F-FDG uptake in organs and tissues measured by dynamic whole body multiparametric FDG PET in 126 patients. EJNMMI Research, 2022, 12, 15.	2.5	17
50	ISSLS Prize Winner: Positron Emission Tomography and Magnetic Resonance Imaging for Monitoring Interbody Fusion With Equine Bone Protein Extract, Recombinant Human Bone Morphogenetic Protein-2, and Autograft. Spine, 2008, 33, 2683-2690.	2.0	16
51	Successful Prediction of Positron Emission Tomography–Imaged Metformin Hepatic Uptake Clearance in Humans Using the Quantitative Proteomics–Informed Relative Expression Factor Approach. Drug Metabolism and Disposition, 2020, 48, 1210-1216.	3.3	15
52	The pathophysiology of Wilson's disease visualized: AÂhuman 64Cu PET study. Hepatology, 2022, 75, 1461-1470.	7.3	15
53	Metabolic liver function measured in vivo by dynamic 18F-FDGal PET/CT without arterial blood sampling. EJNMMI Research, 2015, 5, 32.	2.5	13
54	Metabolic liver function in humans measured by 2-18F-fluoro-2-deoxy-D-galactose PET/CT–reproducibility and clinical potential. EJNMMI Research, 2017, 7, 71.	2.5	12

#	Article	IF	CITATIONS
55	NMDA receptor ion channel activation detected in vivo with [¹⁸ F]GE-179 PET after electrical stimulation of rat hippocampus. Journal of Cerebral Blood Flow and Metabolism, 2021, 41, 1301-1312.	4.3	12
56	Hepatic ethanol elimination kinetics in patients with cirrhosis. Scandinavian Journal of Gastroenterology, 2009, 44, 867-871.	1.5	11
57	Activation of NMDA receptor ion channels by deep brain stimulation in the pig visualised with [18F]GE-179 PET. Brain Stimulation, 2020, 13, 1071-1078.	1.6	11
58	The Holocene dynamics of Ryder Glacier and ice tongue in north Greenland. Cryosphere, 2021, 15, 4073-4097.	3.9	11
59	PET neuroimaging of [11C]mirtazapine enantiomers in pigs. European Neuropsychopharmacology, 2006, 16, 350-357.	0.7	10
60	Hepatic microcirculation assessed by positron emission tomography of first-pass ammonia metabolism in porcine liver. Liver International, 2005, 25, 171-176.	3.9	9
61	Hepatic Blood Perfusion Estimated by Dynamic Contrast-Enhanced Computed Tomography in Pigs. Investigative Radiology, 2012, 47, 588-595.	6.2	9
62	The potential of hyperpolarized ¹³ C magnetic resonance spectroscopy to monitor the effect of combretastatin based vascular disrupting agents. Acta Oncológica, 2017, 56, 1626-1633.	1.8	9
63	Analogue tracers and lumped constant in capillary beds. Journal of Theoretical Biology, 2011, 285, 177-181.	1.7	6
64	FDG-PET reproducibility in tumor-bearing mice: comparing a traditional SUV approach with a tumor-to-brain tissue ratio approach. Acta Oncológica, 2017, 56, 706-712.	1.8	6
65	Human biodistribution, dosimetry, radiosynthesis and quality control of the bile acid PET tracer [N-methyl-11C]cholylsarcosine. Nuclear Medicine and Biology, 2019, 72-73, 55-61.	0.6	6
66	Quantitative PET of liver functions. American Journal of Nuclear Medicine and Molecular Imaging, 2018, 8, 73-85.	1.0	6
67	Clinical feasibility and impact of data-driven respiratory motion compensation studied in 200 whole-body 18F-FDG PET/CT scans. EJNMMI Research, 2022, 12, 16.	2.5	6
68	In vivo vesicular acetylcholine transporter density in human peripheral organs: an [18F]FEOBV PET/CT study. EJNMMI Research, 2022, 12, 17.	2.5	6
69	Renal PET-imaging with 11C-metformin in a transgenic mouse model for chronic kidney disease. EJNMMI Research, 2016, 6, 54.	2.5	5
70	Hypoxia positron emission tomography imaging: combining information on perfusion and tracer retention to improve hypoxia specificity. Acta Oncológica, 2017, 56, 1583-1590.	1.8	5
71	Prevalence of skull pathologies in European harbor seals (Phoca vitulina) during 1981–2014. Mammal Research, 2018, 63, 55-63.	1.3	5
72	Magnetic resonance imaging and computed tomography as tools for the investigation of sperm whale (Physeter macrocephalus) teeth and eye. Acta Veterinaria Scandinavica, 2017, 59, 38.	1.6	4

#	Article	IF	CITATIONS
73	A microvascular compartment model validated using 11C-methylglucose liver PET in pigs. Physics in Medicine and Biology, 2018, 63, 015032.	3.0	4
74	Muscle Tissue Saturation Compared With Muscle Tissue Perfusion During Low Blood Flows: An Experimental Study. Journal of Cardiothoracic and Vascular Anesthesia, 2017, 31, 2065-2071.	1.3	3
75	Metformin is distributed to tumor tissue in breast cancer patients in vivo: A 11C-metformin PET/CT study. Breast Cancer Research and Treatment, 2020, 181, 107-113.	2.5	3
76	Hepatic bile acid transport increases in the postprandial state: AÂfunctional 11C-CSar PET/CT study in healthy humans. JHEP Reports, 2021, 3, 100288.	4.9	3
77	PET kinetics of radiolabeled antidepressant, [N-methyl-11C]mirtazapine, in the human brain. EJNMMI Research, 2011, 1, 36.	2.5	2
78	2-[18 F]fluoro-2-deoxy- D -galactose PET/CT of hepatocellular carcinoma is not improved by co-administration of galactose. Nuclear Medicine and Biology, 2016, 43, 577-580.	0.6	2
79	Cerebral blood flow measured by positron emission tomography during normothermic cardiopulmonary bypass: an experimental porcine study. Perfusion (United Kingdom), 2018, 33, 346-353.	1.0	2
80	Monitoring variables affecting positron emission tomography measurements of cerebral blood flow in anaesthetized pigs. Acta Veterinaria Scandinavica, 2018, 60, 17.	1.6	2
81	Benefits and risks of transforming data from dynamic positron emission tomography, with an application to hepatic encephalopathy. Journal of Theoretical Biology, 2009, 256, 632-636.	1.7	1
82	Model-independent plot of dynamic PET data facilitates data interpretation and model selection. Journal of Theoretical Biology, 2012, 295, 1-8.	1.7	1
83	Reply. Hepatology, 2013, 58, 833-834.	7.3	1
84	Validation and optimisation of an automatic blood sampler for preclinical positron emission tomography research in domestic pigs. Laboratory Animals, 2022, 56, 287-291.	1.0	1
85	Reply to: "Hepatic bile acid transport increases in the postprandial state: A functional 11C-CSar PET/CT study in healthy humansâ€: JHEP Reports, 2021, 3, 100383.	4.9	0